Hydrogen Permeance and Surface States of Pd-Ag/Ceramic Composite Membranes

Li Yang, Zhengxi Zhang, Bingjia Yao, and Xuhui Gao
School of Chemistry and Chemical Technology, Shanghai Jiao Tong University, Shanghai 200240, China

Hitoshi Sakai and Tomonori Takahashi
NGK Insulator Ltd., Mizuho-ku, Nagoya 467-8530, Japan

DOI 10.1002/aic.10892
Published online May 15, 2006 in Wiley InterScience (www.interscience.wiley.com).

Hydrogen permeance and surface states of Pd-Ag/ceramic composite membranes during preparation process were investigated. After thermal treatment in air, the composite membranes exhibited high hydrogen permeability and permselectivity. The sealing process did not change the states of Pd, Ag and O, although an X-ray photoelectron spectroscopic (XPS) signal of sulfide was found. At the same time, the sealing process led to an increase in concentration of carbon and sulfur contaminants in the surface layer, resulting in a decrease of hydrogen permeability. Moreover, carbon was present as graphite and covered membrane surfaces after running the sealing process six times. On the other hand, the thermal treatment in air led to oxidization of Pd and formation of the PdO state, and XPS data showed a significant enrichment of the Pd element at the surface of membranes. Carbon contamination concentration at the top surface of membranes decreased during thermal treatment, and carbon dioxide was found on the surface of activated membranes; at the same time, the surface state of sulfur changed to a new state of sulfate, which eventually resulted in recovery of hydrogen permeability. © 2006 American Institute of Chemical Engineers *AIChE J,* 52: 2783–2791, 2006
Keywords: Pd-Ag composite membranes, gas separation, hydrogen permeance, surface states, XPS

Introduction

Palladium-based membranes have been studied extensively because of their extremely high hydrogen permselectivity and potential in membrane reactors.[1] As has been well established, the promising economy of palladium-based membranes depends on the permeate flux. Much effort has been devoted to improving the hydrogen permeability of palladium-based membranes either by (1) preparation of palladium composite membranes by depositing a thin palladium layer on porous supports such as glass,[2] ceramic,[3-7] and other metals,[8-10] which provide good mechanical strength and thermal stability for the membranes; or (2) using different deposition techniques, such as electroless deposition,[2,5,6,8,9,11] electrodeposition,[10] sputter deposition,[12] and chemical vapor deposition.[3,13] For example, a composite membrane composed of palladium on a porous glass tube was prepared by means of electroless deposition, and the membrane yields greater hydrogen permeability compared to that of commercial palladium membranes. In addition, for the same purpose, several activation methods[14-16] and new fabrication technology[17,18] were also used. For instance, using microsystem technology, Keurentjes et al.[18] produced Pd and Pd/Ag alloy membranes that exhibited fluxes about tenfold higher than those of Pd and Pd/Ag membranes deposited on porous substrates.

In spite of extensive research regarding hydrogen permeabil-

Correspondence concerning this article should be addressed to L. Yang at liyangce@sjtu.edu.cn.

ity for palladium-based membranes, little work has been reported in the following two areas: (1) surface state of Pd-based membranes during fabrication process and (2) relationship between surface state of the membranes and their hydrogen permeability. Detailed investigation on these two aspects can systematically elucidate the physicochemical properties of the Pd-based membranes, and may bring about the discovery of novel metal composite membranes that provide higher hydrogen permeate flux. We previously studied changes in the structure and composition of the top surface of Pd-Ag/ceramic membranes after thermal treatment.[7] It is clear that besides thermal treatment, the high-temperature sealing process is also very important for the gas separation membranes. In this article, we mainly focus on the study of changes in the surface state of the Pd-Ag/ceramic composite membranes during the high-temperature sealing process, using an X-ray photoelectron spectroscopic (XPS) technique, and the influence of these changes on hydrogen permeability. In addition, we also evaluate the hydrogen flux and selectivity at different temperatures and transmembrane pressure differences using pure hydrogen and gas mixtures of H_2/CO_2, H_2/CH_4, H_2/CO, and $H_2/CO_2/CH_4/CO$, and perform the poisoning study of the membrane by introducing 5 ppm H_2S in hydrogen.

Experimental

Membrane preparation

The membranes were prepared by depositing thin and continuous Pd-Ag film on the outside surface of an asymmetric, tubular porous alumina substrate (17 mm OD $\times$ 1040 mm long; NGK Insulator, Ltd.), as shown in Figure 1. Subsequently, porous alumina substrates and permalloy (Fe–45 wt % Ni) flanges were joined by a eutectic alloy of the Ag–Cu system, whose melting point is 1053 K. To decrease the thermal expansion of Ag-based brazing metal, nickel mesh (150 mesh), a low thermal expansion material, was inserted in the brazing metal. The thermal expansion coefficient of the joining material is 13×10^{-6}/K, and the schematic drawing of the joining method is shown in Figure 2. Finally, thermal treatment of the membranes was conducted at 573 K in the air atmosphere for 1 h.

Membrane testing

The composite membranes were tested with pure hydrogen and gas mixtures of H_2/CO_2, H_2/CH_4, H_2/CO, $H_2/CO_2/CH_4/CO$, and H_2/H_2S in the temperature range of 573–773 K to determine the hydrogen permeability and permselectivity. The gas permeation apparatus, as shown in Figure 3, was used to evaluate the permeation properties of the membranes. The hydrogen gas used was ultrahigh-purity grade (99.9999+%); all other gases were used without further purification and have contamination levels in the parts per million (ppm) range. The effective area for hydrogen separation was about 106 cm^2. The pressure outside the membrane varied from 0.2 to 0.9 MPa, whereas the inside was maintained at atmospheric pressure. The pressure was measured by digital pressure gauges made by Keyence Corp. (Shanghai, China). The permeated and residual stream flow rates were measured using a bubble flow meter, and gas stream compositions were analyzed with a gas chromatograph (GC; Model 6890, Hewlett–Packard, Palo Alto, CA).

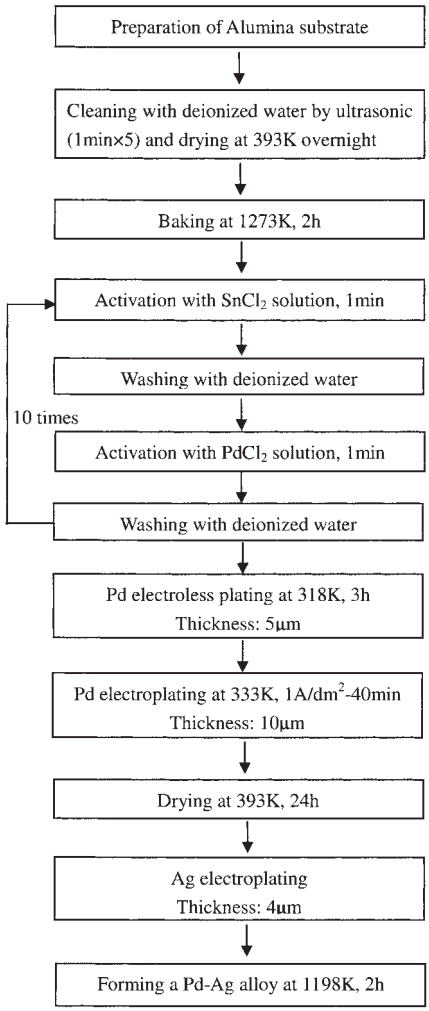

Figure 1. Preparation procedure of Pd-Ag/ceramic composite membranes.

Membrane characterization

Scanning electron microscopic (SEM) photomicrographs of membranes were observed by use of a JSM-T220A scanning electron microscope (JEOL Datum Ltd., Tokyo, Japan). Energy-dispersion X-ray analysis (EDXA) was performed on a JEOL JSM 35CF spectrometer. Chemical compositions of the membrane surfaces were determined by a ESCA-5700ci X-ray photoelectron spectroscopy (XPS; Physical Electronics, Inc., Chanhassen, MN) using α-radiation (300 W) as the exciting source. The analyzed sample area was an 800-μm circle, and the analyzed mode was high-resolution mode (pass energy: 23.5 eV). The rate of Ar ion-sputter etching (3 kV) was 37 Å/min (SiO_2).

Results

Micrography

Figure 4 shows SEM photomicrographs of the surface and fractured cross section of a Pd-Ag/ceramic composite mem-

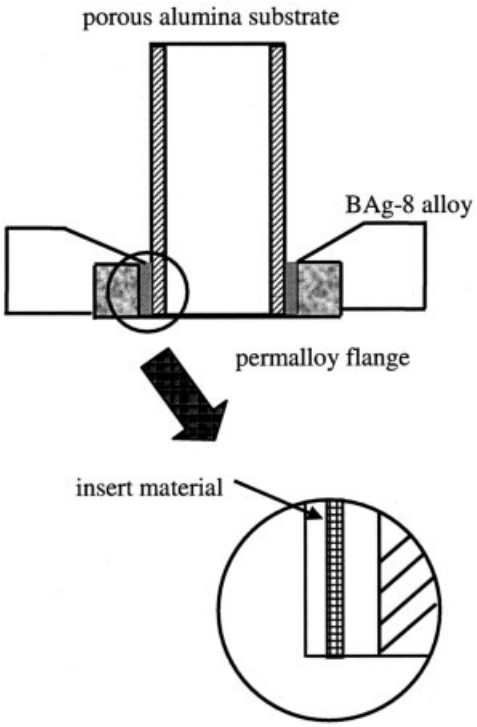

Figure 2. Porous alumina substrate/permalloy flange joint.

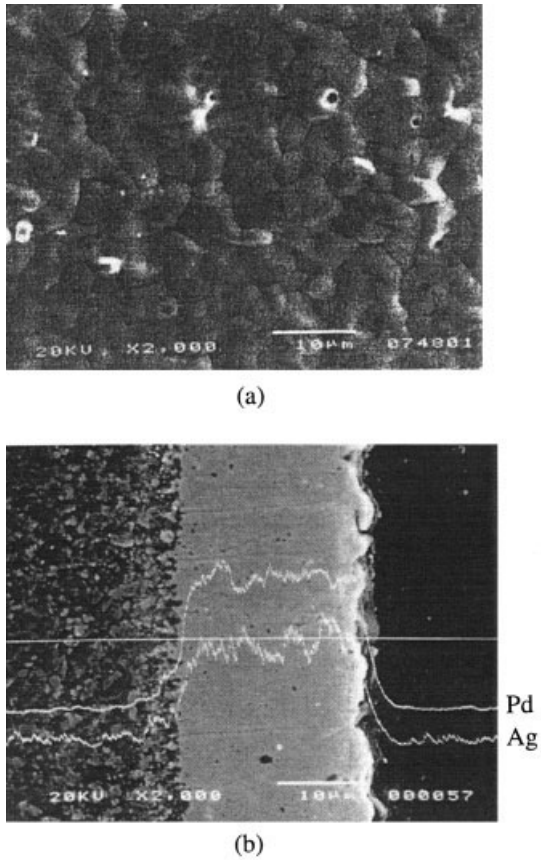

Figure 4. SEM photomicrographs of the surface (a) and cross section (b) of a Pd-Ag/ceramic composite membrane.

brane. From Figure 4a, one observes that the membrane exhibited a homogeneous and nonporous surface. As shown in Figure 4b, the Pd-Ag alloy layer was defect-free and had an almost uniform thickness of about 20 μm. In addition, EDX peaks of Pd and Ag, also appeared in Figure 4b, indicated that both Pd and Ag were distributed homogeneously in the membrane. Moreover, from Figure 5, it was found that silver dis-

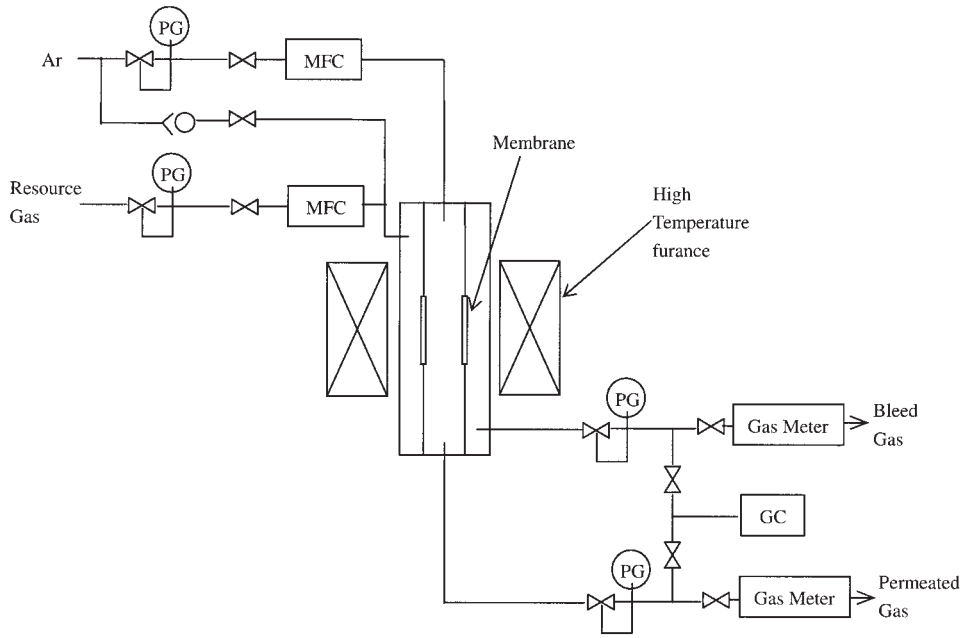

Figure 3. Apparatus used for gas permeation measurement of the membranes.

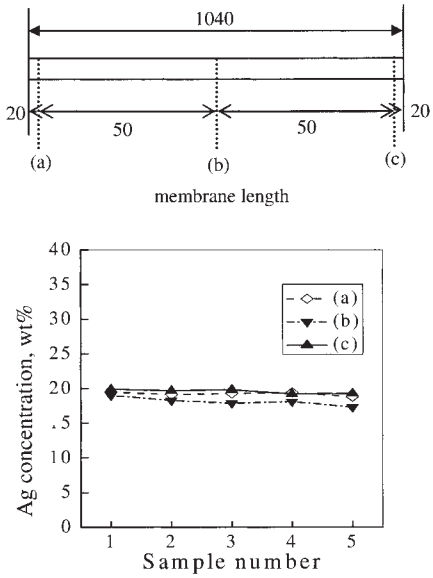

Figure 5. Ag concentration distribution data of Pd-Ag/ceramic membranes.

tribution in the alloy was homogeneous and the average silver concentration was around 20 wt %.

To efficiently separate the permeate from the retentate through the composite membranes, the ceramic substrate and permalloy (Fe–45 wt % Ni) flanges used for module housing were connected. In addition, considering that brazing was satisfied with the sealing joint requirement and suitable for the sealing method at elevated temperature, Ag-based brazing metal was used as the sealing material. It has been established that sealing material should have chemical compatibility with the application environment and possess a thermal expansion coefficient closely matching that of the bulk of the substrate so that cracking does not occur.[19] Therefore, it is essential to decrease the thermal expansion of the brazing metal. In this work, decreasing of the brazing metal thermal expansion was conducted by insertion of a nickel mesh, a low thermal expansion material; the SEM photomicrograph of the cross section of the joints with inserted Ni mesh is shown in Figure 6. Ni mesh was located in the center of clearance. Insertion of Ni mesh was effective in reducing the residual stress in the ceramic substrate. No cracks in the ceramic substrate occurred and good tightness was obtained under 10^{-9} Pa m^3/s of helium leak rate.

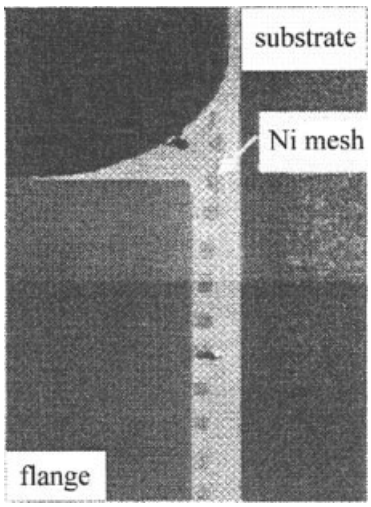

Figure 6. SEM photomicrograph of the joints with inserted Ni mesh.

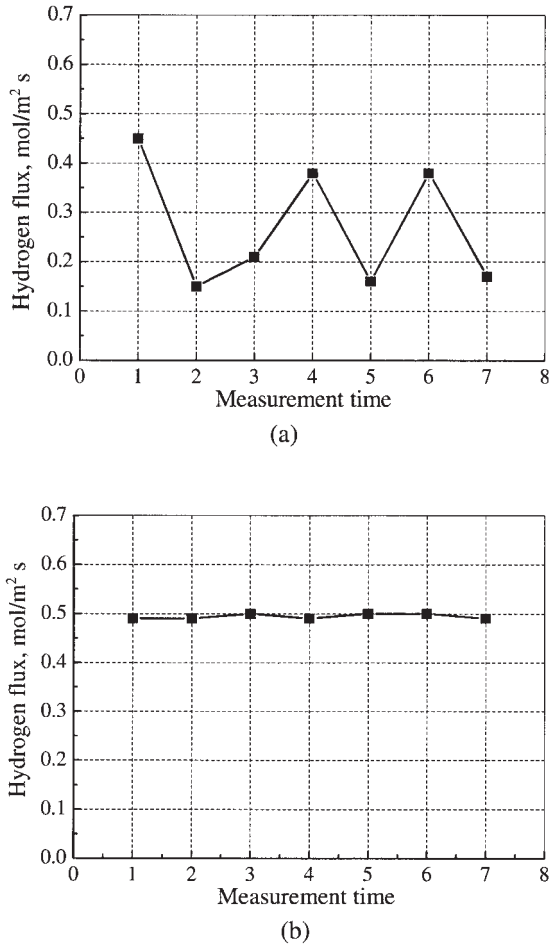

Figure 7. Hydrogen permeability of the membrane.

(a) Before thermal treatment; (b) after thermal treatment.

Hydrogen permeability and selectivity

The hydrogen flux of a composite membrane before and after thermal treatment is shown in Figure 7. For sealed but nonthermally activated membrane, hydrogen permeability was unstable and scattered considerably; however, it was found that hydrogen flux recovered and remained nearly stable after thermal treatment. Thus, thermal treatment had a marked effect for hydrogen permeability of the composite membrane. The composite membranes studied below were all through thermal activation treatment, unless otherwise noted.

Figure 8 shows the permeability of pure hydrogen through Pd-Ag/ceramic composite membranes as a function of the pressure difference at different temperatures. In all cases, the hydrogen flux was proportional to the difference in the square root of pressure, indicating that this agreed with Sievert s law expressed as follows, and the diffusion of hydrogen in the membrane was the rate-determining step:

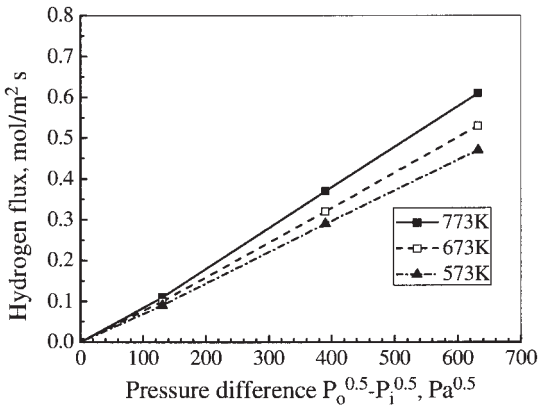

Figure 8. Hydrogen flux through composite membranes as a function of the difference between the square root of the hydrogen pressures on the outer and inner surfaces of the membrane when using pure hydrogen.

$$J = \frac{Q}{t}\left(P_o^{0.5} - P_i^{0.5}\right) \tag{1}$$

$$Q = D_0 S \exp\left(\frac{-E_a}{RT}\right) \tag{2}$$

where J is hydrogen flux; Q is the hydrogen permeation coefficient; D_0 and S are hydrogen diffusivity and hydrogen solubility, respectively; P_o and P_i are the partial pressures of hydrogen on the outer and inner surfaces of the membrane, respectively; t is membrane thickness; and E_a is the apparent activation energy for hydrogen permeation.

Arrhenius relationships between hydrogen permeation coefficient and reciprocal temperature at different pressures are shown in Figure 9. The apparent activation energy values for hydrogen permeation (E_a) were 3.60, 4.44, and 4.71 kJ/mol, corresponding to pressure outside the membrane of 0.2, 0.5, and 0.9 MPa, respectively, which were within the ranges of earlier reported values for the Pd-Ag alloy membranes.[1,20,21]

Considering the steam-reforming reaction of methane (CH_4), binary gas mixtures of H_2/CO_2, H_2/CH_4, and H_2/CO were used to examine the hydrogen permselectivity of the membranes. Very low concentrations of different gases other than hydrogen at different temperatures were detected, and the concentration values for CO_2, CH_4, and CO were about 0.05, 2.90, and 0.05 ppm, respectively.

Hydrogen fluxes and recovery ratios for the above-cited gas mixtures across the membranes at given temperatures are summarized in Table 1. Hydrogen recovery ratio can be expressed as

$$\eta = \frac{JS}{V_0 C_0} \tag{3}$$

where η is hydrogen recovery ratio, J is hydrogen flux, V_0 is resource gas amount, and C_0 is concentration of hydrogen in resource gas.

In the cases of H_2/CO_2 and H_2/CH_4, hydrogen fluxes through membranes decreased as the concentration of CO_2 or CH_4 increased, which can be attributed to the decrease in the hydrogen concentration in the mixture gases. For H_2/CO, a similar result was obtained at 773 K, although, when the temperature decreased to 573 K and CO content was 25%, hydrogen flux decreased rapidly. This could be explained by the fact that CO adsorption on the Pd-Ag alloy surface at comparatively lower temperature led to an obvious decrease of membrane effective area, which then resulted in the deterioration of hydrogen permeability.[21,22]

A mixture of $H_2/CH_4/CO/CO_2$ (70.2:13.5:14.3:2, concentration ratio) was also selected to investigate the hydrogen permselectivity and permeation. CH_4, CO, and CO_2 detected in the permeated gas in the temperature range of 573–773 K had almost the same concentrations as those for the above-mentioned binary mixtures. Figure 10 shows the dependency of hydrogen flux as a function of the difference in the square root of the hydrogen partial pressure at given temperatures. Under the same hydrogen pressure, the permeation flux of hydrogen in the mixture gas was less than that of pure hydrogen. This was attributed to variation in the partial pressure of hydrogen in the mixture gas with hydrogen permeating through the membrane.

In addition, 5 ppm H_2S in hydrogen was used to examine the effect of H_2S poisoning on the hydrogen flux of the membrane at 773 K and 0.8 MPa transmembrane pressure, and the result is presented in Figure 11. Once 5 ppm hydrogen sulfide (H_2S) was introduced in pure hydrogen, the hydrogen flux decreased to 16.7% of the original value. When pure hydrogen was reintroduced, the hydrogen flux was an almost 100% recovery of the original value, which indicated that a very small amount of hydrogen sulfide (H_2S) adsorbed onto the Pd-Ag alloy surface could lead to a substantial decrease in the hydrogen flux.[22-24]

XPS results

XPS spectra of the surface of Pd-Ag/ceramic composite membranes are shown in Figure 12, which revealed that the impurities of carbon, oxygen, sulfur, chlorine, and sodium were present besides palladium and silver. The relative content of the membrane surface composition can be obtained by means of calculating the corresponding area of XPS spectra humps, the quantitative results of which are presented in Figure 13.

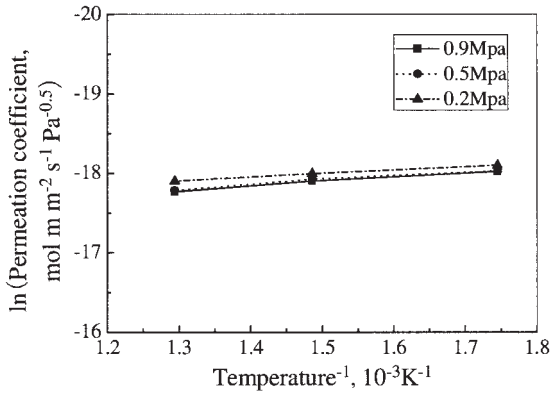

Figure 9. Temperature dependency of permeation coefficient.

Table 1. Hydrogen Fluxes and Recovery Ratio for Gas Mixtures

		Gas Mixtures								
		H_2/CO_2 CO_2 concentration (%)			H_2/CH_4 CH_4 concentration (%)			H_2/CO CO concentration (%)		
T (K)	Pure H_2	1	10	25	1	10	25	1	10	25
773	0.68	0.66*	0.58	0.47	0.66	0.58	0.46	0.65	0.57	0.45
		(46)**	(43)	(42)	(45)	(44)	(40)	(42)	(40)	(39)
673	0.60	0.58	0.51	0.41	0.58	0.51	0.42	0.56	0.50	0.37
		(40)	(39)	(37)	(39)	(38)	(36)	(36)	(34)	(31)
573	0.59	0.58	0.50	0.40	0.57	0.50	0.41	0.51	0.38	0.15
		(40)	(37)	(35)	(39)	(37)	(34)	(29)	(24)	(12)

*Hydrogen flux (mol m^{-2} s^{-1}).
**Recovery ratio (%).

The carbon concentration on the top surface of sample c was less than that of either sample a or sample b. Moreover, from the O KLL peak, we could see that compared with silver concentration, concentrations of palladium and oxygen relatively increased. For the sample before thermal treatment (sample b), the Ag/Pd ratio was about 1:2.5, which agreed with the results from other researchers[25-27] and was higher than the target ratio (Ag/Pd = 1:3.4), suggesting a silver enrichment at the top surface of the membrane. After thermal treatment (sample c), the Ag/Pd ratio changed from 1:2.5 to 1:3.4, indicating a diffusion of palladium toward the top surface during thermal treatment. In addition, it could not be found that sulfur, chlorine, and sodium existed in the inside of the membranes, revealing that they were present only in the outermost layer. In particular, compared to nonsealed membranes, the sulfur concentration on the top surface increased after the sealing process, which can be attributed to the atmosphere during the sealing process and thermal history during electroplating. After sealing for six times, copious amounts of carbon were present, and nearly covered the top surface of the membranes.

The high-resolution XPS spectra of the elements and their states are shown in the following:

Ag3d Region. The high-resolution signals of the Ag3d region are shown in Figure 14. Ag was in a state of Ag-Pd alloy before and after the sealing process; after thermal treatment, the Ag3d peak broadened, revealing that minor Ag was oxidized. This indicated the presence of minor Ag oxide, in addition to major metallic silver.

Pd3d Region. The high-resolution spectra of the Pd3d region (Figure 15) showed that Pd existed as Ag-Pd alloy and PdO_x ($0 < x < 1$) states before and after the sealing process; after thermal treatment, for sample c, the main peak on the XPS spectrum of Pd3d shifted to higher binding energy, which was the position of the peak of PdO. This revealed that during thermal treatment in the air atmosphere, palladium was further oxidized, and PdO was formed, which could be attributed to O species associated with the PdO_x. Therefore, Pd was present as Ag-Pd alloy and PdO states after thermally activated treatment. In addition, for sample e, no peaks were found corresponding to PdO_x or PdO, indicating that PdO_x or PdO was present only on the top surface.

C1s Region. C1s XPS high-resolution spectra are shown in Figure 16. C was present as C—C, C—O, and C—OO bonding before and after the sealing process; after thermal treatment, carbon concentration decreased as a result of carbon decomposition, which could be verified by the appearance of a new peak corresponding to CO_2 species. In addition, C exhibited a graphite structure after being sealed for six times.

O1s Region. O1s XPS high-resolution spectra are shown in Figure 17. The O1s peak overlapped with the $Pd3d_{3/2}$ signal, with the result that the O1s peak could not observed; however, after thermal treatment in air atmosphere, the O1s peak could be distinguished from the broad $Pd3d_{3/2}$ peak, which was attributed to an increase of the peak width. This indicated

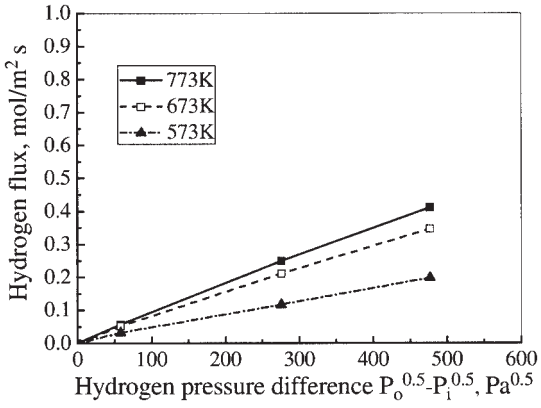

Figure 10. Hydrogen flux through composite membranes as a function of the difference between the square root of the hydrogen partial pressures on the outer and inner surfaces of the membrane when using gas mixture of H_2/CH_4/CO/CO_2.

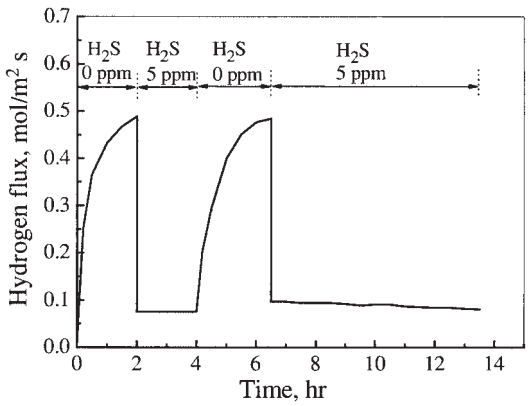

Figure 11. Hydrogen flux after poisoning by 5 ppm hydrogen sulfide and hydrogen recovery.

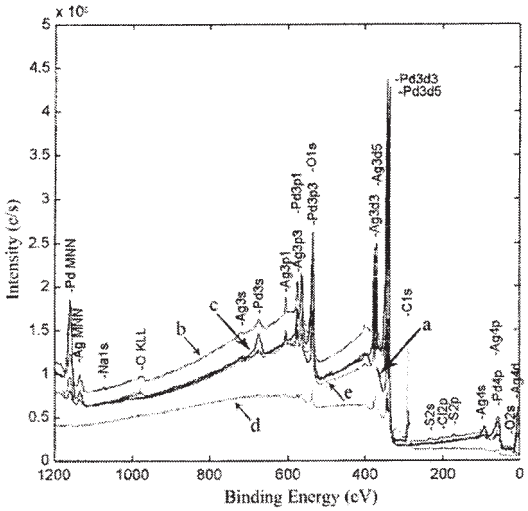

Figure 12. XPS spectrum of Pd-Ag/ceramic membranes.

(a) Before sealing; (b) after sealing for two times; (c) after thermal treatment; (d) after sealing for six times; (e) etched surface at a depth of about 800Å below the top surface.

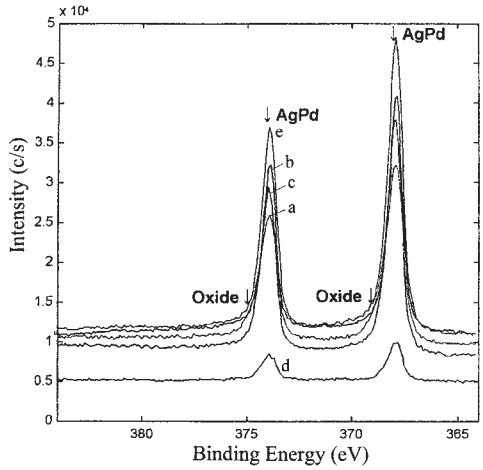

Figure 14. Ag 3d XPS high-resolution spectra of membranes.

(a) Before sealing; (b) after sealing for two times; (c) after thermal treatment; (d) after sealing for six times; (e) etched surface at a depth of about 800 Å below the top surface.

growth of the oxide layer on the top surface of alloy during the thermal treatment.

S2p Region. S2p XPS high-resolution spectra are shown in Figure 18. Before sealing, S existed as sulfur (S) or sulfide (S^{2-}); after sealing process, S was present as sulfide (S^{2-}) and sulfate (SO_4^{2-}); after thermal treatment, S was present only as sulfate state (SO_4^{2-}), indicating that S was oxidized and changed to a new state of sulfate (SO_4^{2-}) in the air atmosphere.

Valence Band Region. The valence bands of all the samples studied are shown in Figure 19. The peaks corresponding to Ag and Pd appeared around 3–5 and 0–3 eV, respectively; after thermal treatment, the valence band energy changed as a result of the oxidization of Pd. In addition, The O2s peak shift was observed as a result of formation of PdO.

Discussion

The concentration of carbon contaminant in the surface layer decreased, and sulfur was oxidized after thermal treatment. Carbon contaminants covering the surface layer of Pd-Ag membranes not only hindered the reaction between hydrogen and membranes, but also induced the reaction between carbon and hydrogen, leading to formation of methane, which eventually decreased hydrogen permeability. In addition, sulfur can react with hydrogen and the anticipated product is hydrogen sulfide gas. Experimental results showed that addition of only 5 ppm hydrogen sulfide in hydrogen resulted in an obvious decrease of hydrogen permeability; however, reintroducing pure hydrogen can recover permeability, indicating that sulfur—which existed in the top layer—was one of the main reasons for decreasing hydrogen permeability. At the same time, hydrogen permeability could be recovered after thermal treatment in air atmosphere, which can be explained by the following two points: (1) carbon contaminant on the surface

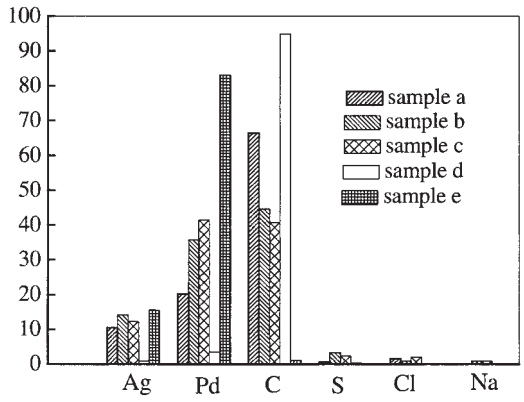

Figure 13. Surface atomic percentage measured on top surface and etched surface at a depth of about 800 Å below the top surface.

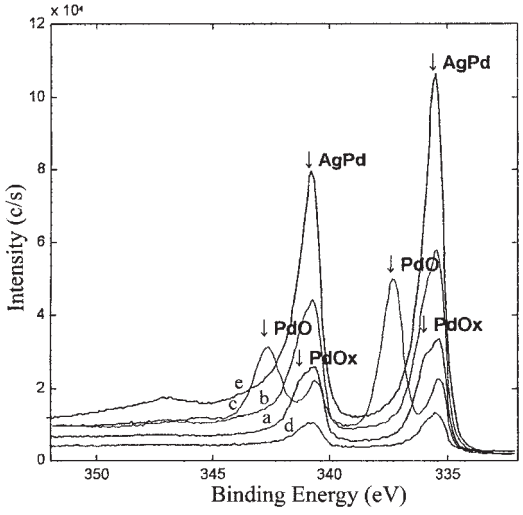

Figure 15. Pd3d XPS high-resolution spectra of membranes.

(a) Before sealing; (b) after sealing for two times; (c) after thermal treatment; (d) after sealing for six times; (e) etched surface at a depth of about 800 Å below the top surface.

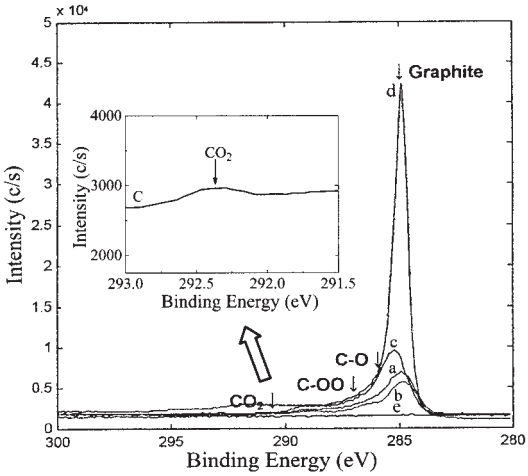

Figure 16. C1s XPS high-resolution spectra of membranes.

(a) Before sealing; (b) after sealing for two times; (c) after thermal treatment; (d) after sealing for six times; (e) etched surface at a depth of about 800 Å below the top surface.

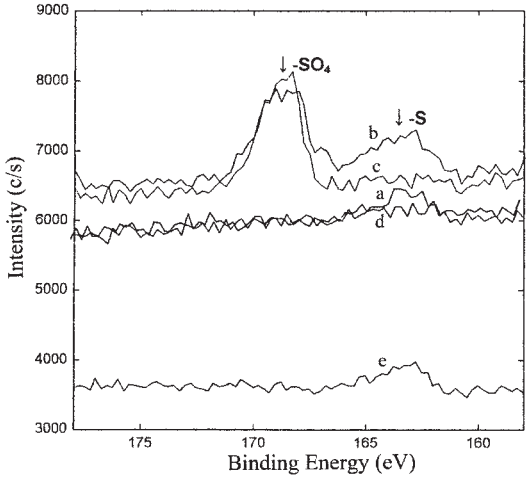

Figure 18. S2p XPS high-resolution spectra of membranes.

(a) Before sealing; (b) after sealing for two times; (c) after thermal treatment; (d) after sealing for six times; (e) etched surface at a depth of about 800 Å below the top surface.

layer changed to CO and CO_2 during the combustion process and, as a result, contaminate concentration at the surface layer decreases; (2) sulfide (S^{2-}) was oxidized and yielded sulfate (SO_4^{2-}) during the combustion process, which hindered the formation of hydrogen sulfide gas. In addition, large amounts of graphite exist at the top surface of membranes after running the sealing process for six times, which could be mainly attributed to the sealing atmosphere.

Conclusions

In this study, changes in the surface state of Pd-Ag/ceramic composite membranes during the fabrication process, especially the high-temperature sealing process, were investigated. Hydrogen permeability and selectivity were also evaluated at various temperatures and transmembrane pressure differences. The conclusions can be summarized as follows:

(1) The composite membranes exhibited both a high hydrogen flux and permselectivity.

(2) Carbon contamination content at the top surface of membranes decreased during thermal treatment, and CO_2 was found on the surface of thermally activated membranes.

(3) Thermal treatment resulted in oxidization of Pd and formation of PdO. Moreover, an obvious enrichment of Pd element was found on the surface of treated membranes.

(4) Sulfur existed in a state of sulfide (S), sulfur (S^{2-}), and sulfate (SO_4^{2-}) before the sealing process, after the sealing process, and after thermal treatment, respectively.

(5) Composite membranes surface were extensively covered by graphite after running the sealing process for six times.

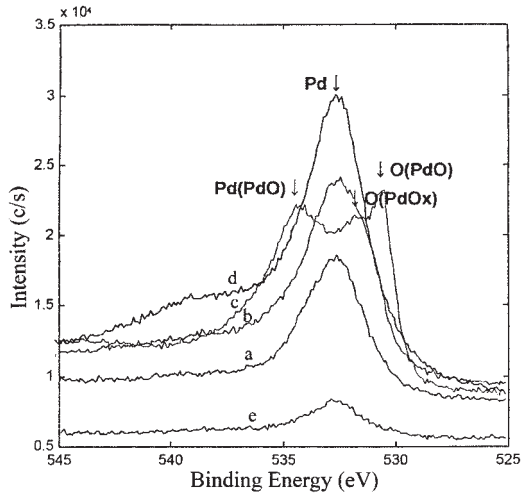

Figure 17. O1s XPS high-resolution spectra of membranes.

(a) Before sealing; (b) after sealing for two times; (c) after thermal treatment; (d) after sealing for six times; (e) etched surface at a depth of about 800 Å below the top surface.

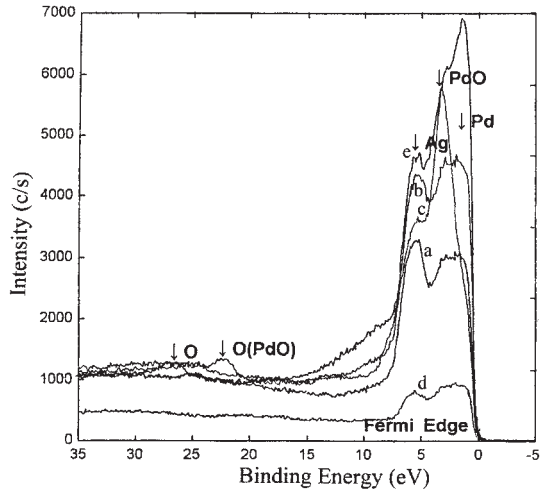

Figure 19. Valence bands of membranes.

(a) Before sealing; (b) after sealing for two times; (c) after thermal treatment; (d) after sealing for six times; (e) etched surface at a depth of about 800 Å below the top surface.

Acknowledgments

This work was sponsored by Shanghai Pujiang Program (05PJ14066). The authors thank Y. Mori for technical assistance with the XPS experiment.

Literature Cited

1. Shu J, Grandjean BPA, Neste AV, Kaliaguine S. Catalytic palladium-based membrane reactors: A review. *Can J Chem Eng.* 1991;69:1036-1060.
2. Uemiya S, Kude Y, Sugino K, Sato N, Matsuda T, Kikuchi E. A palladium/porous-glass composite membrane for hydrogen separation. *Chem Lett.* 1988;10:1687-1690.
3. Uemiya S, Matsuda T, Kikuchi E. Hydrogen permeable palladium-silver alloy membrane supported on porous ceramics. *J Membr Sci.* 1991;56:315-325.
4. Soria R. Overview on industrial membranes. *Catal Today.* 1995;25: 285-290.
5. Roa F, Way JD. Influence of alloy composition and membrane fabrication on the pressure dependence of the hydrogen flux of palladium-copper membranes. *Ind Eng Chem Res.* 2003;42:5827-5835.
6. Tanaka DAP, Tanco MAL, Niwa SI, Wakui Y, Mizukami F, Namba T, Suzuki TM. Preparation of palladium and silver alloy membrane on a porous α-alumina tube via simultaneous electroless plating. *J Membr Sci.* 2005;247:21-27.
7. Yang L, Zhang ZX, Gao XH, Guo YJ, Wang BF, Sakai O, Sakai H, Takahashi T. Changes in hydrogen permeability and surface state of Pd-Ag/ceramic composite membranes after thermal treatment. *J Membr Sci.* 2005;252:145-154.
8. Shu J, Grandjean BPA, Ghali E, Kaliaguine S. Simultaneous deposition of Pd and Ag on porous stainless steel by electroless plating. *J Membr Sci.* 1993;77:181-195.
9. Mardilovich PP, She Y, Ma YH, Rei MH. Defect-free palladium membranes on porous stainless-steel support. *AIChE J.* 1998;44:310-322.
10. Nam SE, Lee KH. Preparation and characterization of palladium alloy composite membranes with a diffusion barrier for hydrogen separation. *Ind Eng Chem Res.* 2005;44:100-105.
11. Souleimanova RS, Mukasyan AS, Varma A. Pd membrane formed by electroless plating with osmosis: H_2 permeation studies. *AIChE J.* 2002;48:262-268.
12. Jayaraman V, Lin YS, Pakala M, Lin RY. Fabrication of ultrathin metallic membranes on ceramic supports by sputter deposition. *J Membr Sci.* 1995;99:89-100.
13. Yan S, Maeda H, Kusakabe K, Morooka S. Thin palladium membrane formed in support pores by metal-organic chemical vapor deposition method and application to hydrogen separation. *Ind Eng Chem Res.* 1994;33:616-622.
14. Roshan NR, Mishchenko AP, Polyakova VP, Parfenova NI, Savitsky EM, Voitekhova EA, Gryaznov VM, Sarylova ME. The effect of the surface state on the hydrogen permeability and catalyst activity of palladium-alloy membranes. *J Less Common Metals.* 1983;89:423-428.
15. Skakunova EV, Ermilova MM, Gryaznov VM. Hydrogenolysis of propane on a Pd-Ru alloy membrane catalyst. *Bull Acad Sci USSR Div Chem Sci.* 1988;37:858-861.
16. Nam SE, Lee KH. A study on the palladium/nickel composite membrane by vacuum electrodeposition. *J Membr Sci.* 2000;170:91-99.
17. Tong HD, Gielens FC, Gardeniers JGE, Jansen HV, Rijn CJMV, Elwenspoek MC, Nijdam W. Microfabricated palladium-silver alloy membranes and their application in hydrogen separation. *Ind Eng Chem Res.* 2004;43:4182-4187.
18. Keurentjes JTF, Gielens FC, Tong HD, Rijn CJMV, Vorstman MAG. High-flux palladium membranes based on microsystem technology. *Ind Eng Chem Res.* 2004;43:4768-4772.
19. Hsieh HP. *Inorganic Membranes for Separation and Reaction*. Amsterdam, The Netherlands: Elsevier; 1996.
20. Ali JK, Newson EJ, Rippin DWT. Deactivation and regeneration of Pd-Ag membranes for dehydrogenation reactions. *J Membr Sci.* 1994; 89:171-184.
21. Amandusson H, Ekedahl LG, Dannetun H. Hydrogen permeation through surface modified Pd and PdAg membranes. *J Membr Sci.* 2001;193:35-47.
22. Bryden KJ, Ying JY. Nanostructured palladium–iron membranes for hydrogen separation and membrane hydrogenation reactions. *J Membr Sci.* 2002;203:29-42.
23. Doroshin AY, Livshits AI, Samartsev AA. Interaction of hydrogen atoms with palladium surfaces passivated by adsorbed sulfur layers. *Phys Chem Mech Surf.* 1987;4:2321-2330.
24. Kajiwara M, Uemiya S, Kojima T. Stability and hydrogen permeation behavior of supported platinum membranes in presence of hydrogen sulfide. *Int J Hydrogen Energy.* 1999;24:839-844.
25. Wood BJ, Wise H. Surface composition of Pd-Au and Pd-Ag catalysts by Auger electron spectroscopy. *Surf Sci.* 1975;52:151-160.
26. Schwartz GP. Segregation studies in Pd-Ag. *Surf Sci.* 1978;76:113-129.
27. Reniers F, Jardinier-Offergeld M, Bouillon F. Auger electron spectroscopy study of the surface segregation in silver-palladium alloys. *Surf Interface Anal.* 1991;17:343-351.

Manuscript received Aug. 2, 2005, and revision received Apr. 7, 2006.